cy 1

AEDC-TR-65-148

# LOW DENSITY BOUNDARY LAYER CONTROL BY LIQUID HYDROGEN CYROPUMPING

W. N. MacDermott, R. E. Dix, and B. H. Shirley
ARO, Inc.



August 1965



PROPULSION WIND TUNNEL FACILITY
ARNOLD ENGINEERING DEVELOPMENT CENTER
AIR FORCE SYSTEMS COMMAND
ARNOLD AIR FORCE STATION, TENNESSEE

# NOTICES

When U. S. Government drawings specifications, or other data are used for any purpose other than a definitely related Government procurement operation, the Government thereby incurs no responsibility nor any obligation whatsoever, and the fact that the Government may have formulated, furnished, or in any way supplied the said drawings, specifications, or other data, is not to be regarded by implication or otherwise, or in any manner licensing the holder or any other person or corporation, or conveying any rights or permission to manufacture, use, or sell any patented invention that may in any way be related thereto.

Qualified users may obtain copies of this report from the Defense Documentation Center.

References to named commercial products in this report are not to be considered in any sense as an endorsement of the product by the United States Air Force or the Government.

# LOW DENSITY BOUNDARY LAYER CONTROL BY LIQUID HYDROGEN CRYOPUMPING

W. N. MacDermott, R. E. Dix, and B. H. Shirley
ARO, Inc.

## FOREWORD

The work reported herein was sponsored by the Arnold Engineering Development Center (AEDC), Air Force Systems Command (AFSC), under Program Element 62410034, Project 7778, Task 777805.

The results of the research presented were obtained by ARO, Inc. (a subsidiary of Sverdrup and Parcel, Inc.), contract operator of the AEDC, AFSC, Arnold Air Force Station, Tennessee, under Air Force contract AF 40(600)-1200. The research was conducted from August 1963 to June 1964 under ARO Project Number PL2291, and the manuscript was submitted for publication on June 14, 1965.

The data included herein were presented under the title "Low Density Boundary Layer Control by Liquid Hydrogen Cryopumping" to the Fourth International Symposium on Rarefied Gas Dynamics, held at the University of Toronto, Toronto, Ontario, July 14 through 17, 1964.

This technical report has been reviewed and is approved.

Charles V. Bennett
Project Engineer
Technology Division
DCS/Plans and Technology

Donald D. Carlson
Colonel, USAF
DCS/Plans and Technology

## ABSTRACT

Thick boundary layers in a low density wind tunnel nozzle have been reduced by applying suction on the diverging walls of the nozzle. Extremely high suction rates have been established by cryogenically pumping the boundary layer gas directly to the wall. The experimental apparatus used in this study incorporates a 12-in. -diam hypersonic nozzle and a 16-in. primary liquid hydrogen cryopump with a pumping speed of 200,000 liters/sec. Comparison of pitot and static pressures measured in this nozzle with nitrogen at an upstream settling chamber temperature ($T_{o1}$) of 300°K indicates a supersaturated isentropic flow regime bounded on the low pressure end by a merged boundary layer. In a typical operating condition at $T_{o1}$ = 300°K, a merged boundary layer flow at M = 9.50, Re = 256/cm, and a mean free path of 0.06 cm was converted to a 4-in. core flow with M = 15.7, Re = 40/cm, and a mean free path of 0.6 cm by cooling the nozzle walls sufficiently for initiation of cryopumping. This nozzle has also been supplied with arc-heated nitrogen, and it has been found that the wall cryopumping retains effectiveness at supply temperatures at least as high as 4000°K, although for a lesser period of time and at lower efficiency. When operating this apparatus with an arc heater, evidence has been found that there are some nitrogen atoms formed in the arc discharge which survive the expansion flow through the nozzle and are trapped on the cryogenic surfaces in atomic form.

## CONTENTS



## ILLUSTRATIONS

## NOMENCLATURE

| | |
|---|---|
| D | Nozzle exit diameter |
| d* | Throat diameter |
| $F_V$ | Van Driest (Ref. 2) boundary layer thickness parameter = $\frac{\delta}{x}\sqrt{Re_x}$ |
| Kn | Knudsen number = $L_{mean}/L_c$ |
| $Kn_{cm}$ | Knudsen number for $L_c$ = 1 cm |
| L | Length of nozzle along the wall |
| $L_c$ | Characteristic length |
| $L_{mean}$ | Mean free path = $\frac{32\mu}{5\pi\rho\bar{v}}$ |
| M | Mach number |
| $\dot{m}$ | Mass flux |
| P | Pressure |
| Pr | Prandtl number |
| R | Nozzle exit radius or gas constant |
| Re | Reynolds number |
| T | Temperature |
| $\bar{v}$ | Mean molecular velocity, $\sqrt{\frac{8RT}{\pi}}$ |
| x | Length of developed boundary layer |
| $\delta$ | Boundary layer thickness |
| $\delta^*$ | Boundary layer displacement thickness |
| $\mu$ | Microns of Hg or absolute viscosity |
| $\rho$ | Density |

### SUBSCRIPTS

| | |
|---|---|
| 1 | Static condition at nozzle exit |
| L | Parameter based on nozzle length |
| $L_c$ | Parameter based on characteristic length |

| | |
|---|---|
| $o_1$ | Upstream settling chamber condition |
| $o_2$ | Impact condition at nozzle exit |
| $v_1$ | Cryopump chamber |
| $v_2$ | Nozzle plenum chamber |
| w | Wall condition |
| x | Parameter based on length of developed boundary layer |
| $\infty$ | Free-stream condition |

## SECTION I
## INTRODUCTION

The phenomenon of excessive boundary layer growth in the expansion nozzle of a low density wind tunnel is well known. In the extreme case of a merged boundary layer this growth forms a fundamental limit to low density simulation in such a facility. Early low density wind tunnels frequently operated with a boundary layer thickness ratio, $\delta/R$, in the neighborhood of 0.50, whereas conventional wind tunnels rarely operated with $\delta/R$ much over 0.10. A number of erstwhile conventional facilities are now routinely operated in a low density mode of operation. As the simulated density levels were pushed to lower and lower levels, thicker boundary layers had to be tolerated and in some cases testing was accomplished with $\delta/R$ fairly close to unity (Ref. 1).

To define the low density limit imposed by the boundary layer a simplified analysis of reasonable accuracy is desirable. It has often been found that nozzle boundary layers calculated on the basis of a simple flat plate theory are surprisingly close to experimental measurements. For hypersonic nozzles this is no mere coincidence, since the velocity gradient is large only in the immediate vicinity of the throat; for up to 90 percent of the nozzle length, the velocity gradient is close to the flat plate value and a flat plate solution would naturally provide a good approximation. The exact flat plate solutions of Van Driest (Ref. 2) for a laminar boundary layer with Pr = 0.75 and a Sutherland viscosity law give boundary layer thickness in a simple dimensionless form:

$$\frac{\delta}{x}\sqrt{Re_x} = F_v\left(M_\infty, \frac{T_w}{T_\infty}\right) \tag{1}$$

In Fig. 1, a large amount of experimental nozzle boundary layer thickness data is given as the dimensionless parameter, $\left(\frac{\delta}{L}\sqrt{Re_L}\right)_{exp}$, normalized by the theoretical Van Driest value, $F_V$, plotted as a function of total Reynolds number. It appears that the laminar flat plate approximation is valid for hypersonic nozzles to within ±15 percent for a large range in Mach number and cooling rates, and for $Re_L < 10^5$. All of the data given for $Re_L > 10^5$ are obviously turbulent data.

Using this simple relation for boundary layer growth, the limiting low Reynolds number for merged flow is given as

$$(Re_L)_{merge} = 16\,F_v^2 \tag{2}$$

where it is assumed that $\delta = D/2$ and that $L/D = 2.0$, which is probably a minimum value for hypersonic nozzles and corresponds roughly to a 30-deg

total-angle conical nozzle. This $(Re_L)_{merge}$ is a universal limit for hypersonic nozzles, regardless of size, and is plotted on the upper part of Fig. 2 for the two distinct cases of adiabatic walls and highly cooled walls ($T_w = T_\infty$). Since the $Re_L$ scale is logarithmic, the inaccuracy of the flat plate theory would show up as correspondingly narrow error bands about these two curves. For a given $(Re_L)_{merge}$, it is clear that the minimum attainable unit Reynolds number, an index of the degree of rarefaction, will be inversely proportional to the nozzle scale.

The Reynolds number limit is readily converted to a Knudsen number limit,

$$Kn = \frac{L_{mean}}{L_c} = \frac{32\mu}{5\pi\rho\bar{v}L_c} = 1.512\,\frac{M}{Re_{L_c}} \tag{3}$$

For a characteristic length of one centimeter,

$$(Kn_{cm})_{merge} = 1.512\,\frac{M}{(Re/cm)_{merge}} = 1.512\,\frac{ML}{(Re_L)_{merge}} \tag{4}$$

This $(Kn_{cm})_{merge}$ is a maximum value for hypersonic nozzles and is directly proportional to the nozzle scale. It is plotted in the lower half of Fig. 2 for a 12-in. exit diameter nozzle for the same two conditions of wall cooling as the Reynolds number curves. By definition, this parameter is also the maximum mean free path in centimeters attainable at the boundary layer merge point. For a model length of 1 cm, the maximum Kn in the range of Mach number from 10 to 20 varies from 0.1 to 0.3, well below the free molecule regime. For conventional hypersonic nozzles of 12-in. diameter, then, free molecule conditions can only be achieved with extremely small models. The experimental data on Fig. 2 are discussed later.

The low density limits just derived are for natural boundary layer growth. A number of investigations have been made of the possibility of extending these limits by various means of boundary layer control. Stalder et al. (Ref. 3) and Enkenhus (Ref. 4) describe experimental and theoretical work on establishing boundary layer suction through porous wall nozzles. The conclusion that the supplemental pumping capacity for the suction flow could just as well be added to the primary pumping system to pump a larger nozzle, however, was based on the use of conventional means of pumping the suction flow. The extremely high volumetric pumping capacity of cryogenically cooled plates was early recognized as being especially well suited to provide the primary pumping for low density wind tunnels (Ref. 5). The use of cryogenic pumping for boundary layer control appeared to be a natural extension. The basic feasibility of cryopumping a supersonic low density boundary layer directly to the chilled walls of a M = 3.0 supersonic nozzle was reported by the author (Ref. 6)

for carbon dioxide as a test gas. An alternate technique of using cryogenic pumping in combination with a regular porous wall nozzle was recently investigated by Bottorf and Rogers (Ref. 7). An extension of the author's investigation is reported herein. A more representative test gas (nitrogen) has been used, the Mach number has been increased to the M = 10 range, the test apparatus has been scaled up to a 1-ft diameter, and operation at high stagnation enthalpies has been provided by an arc-heated supply.

## SECTION II
## DESCRIPTION OF TEST FACILITY

The test apparatus is shown schematically in Fig. 3. The main components are, from left to right: a 40-kw d-c arc heater, a reservoir chamber with radiation-cooled liner, a 12-in. exit diameter expansion nozzle, instrumentation probes, a primary cryopump, and an auxiliary pumping system.

The nozzle has a throat diameter of 0.150 in. and a conical diverging section with a total expansion angle of 30 deg. From a station 4 in. downstream of the throat at a geometric Mach number of 8.5, to the exit of the nozzle, the diverging wall is surrounded by a coolant jacket. There are four separate jackets which are commonly manifolded together as a single jacket. When liquid hydrogen is used as a coolant, a wall temperature of 20.4°K is produced. Because of the much higher heat transfer rates at the throat, separate cooling is provided in this region. Both water and liquid nitrogen have been used for throat cooling.

The primary cryopump is an annular cylindrical tank 30 in. long and 16 in. in diameter, mounted on knife edge supports in the vacuum tank downstream of the nozzle. It has a surface area of approximately 3000 sq in. and an ideal free molecule pumping speed for nitrogen of 224,000 liters/sec. A 50-cfm mechanical vacuum pump and a 1500-liter/sec oil diffusion pump form the auxiliary pumping system used for initial pumpdown and holding.

Pressures are measured at the points indicated in Fig. 3 with Alphatron® pressure gages. Pitot pressures are measured at the nozzle exit with a five-tube rake. Each probe is connected to a separate gage, but only one is shown for simplicity.

Operation of this facility requires up to 4 kw of refrigeration at a temperature at least as low as 30°K. A closed-loop helium refrigerator could provide this, but the initial cost would be very high (~$400,000). For this reason, an open-cycle system using the latent heat of liquid hydrogen boiling at atmospheric pressure was selected. One gallon of liquid hydrogen

will provide 0.0293 kw-hr of refrigeration at 20.4°K when boiled away to vapor. The current cost of liquid hydrogen is $0.425 per gallon, giving an operating cost of $14.50 per kw-hr of refrigeration. A 40-gal dewar vessel is located outside the test building, and liquid hydrogen is fed to the nozzle jacket and cryopump through a vacuum-insulated supply line. The evolved gaseous hydrogen is vented to the atmosphere at a remote point outside the building through a completely enclosed vent system. The 40-gal local storage capacity is adequate to run the facility for from 30 to 60 minutes, depending upon the mode of operation.

## SECTION III
## TEST RESULTS

The boundary layer control test nozzle has been operated from $T_{o1}$ = 300 to 4000°K. A majority of the results so far obtained have been for $T_{o1}$ = 300°K because of the simplicity of operation and data reduction when operating with an unheated supply gas. These results will be described first, followed by a description of results at higher temperatures with the arc heater in operation.

### 3.1 $T_{o_1}$ = 300°K WITH NATURAL BOUNDARY LAYER

#### 3.1.1 Magnitudes of Measured Pressures

For reservoir pressure ranging from 1 to 730 mm Hg, the nozzle exit pitot pressure $P_{o2}$ is 1 to 500$\mu$, the nozzle exit static pressure is 0.7 to 3$\mu$, the nozzle plenum pressure $P_{v2}$ is 0.07 to 1$\mu$, and the cryopump chamber pressure $P_{v1}$ is 0.002 to 1$\mu$. The $P_{v2}$ is always about 0.3 $P_1$ so that the nozzle is always slightly underexpanded. Measured values of $P_{v1}$ and nozzle mass flow imply an effective pumping speed of 200,000 liters/sec at the cryopump in the free molecule range, which is slightly less than the ideal value of 224,000 liters/sec.

#### 3.1.2 Pitot Pressure Profiles

A family of pitot pressure profiles for eight reservoir pressures is given in Fig. 4. For this hypersonic nozzle the flow is half boundary layer even at atmospheric supply pressure, and the regular incursion of the boundary layer upon the core flow as $P_{o1}$ decreases is observed. Merging of the boundary layers from opposite walls occurs at $P_{o1}$ = 45 mm Hg. There are strong gradients in the core flows, with compression regions near the edges of the cores for $P_{o1}$ between 180 and 730 mm Hg. Since the nozzle is always slightly underexpanded, these

non-uniformities are not related to any compressive adjustment to downstream flow conditions. They are believed to be a result of nonlinear contouring of the conical nozzle by the boundary layer displacement as the Reynolds number decreases. It would be expected that initially the core flow would be a modified spherical source flow with an effective expansion angle slightly less than the nozzle expansion angle, followed by a regime in which compressive disturbances invade the core from the edges as the $\delta^*$ growth becomes large and nonlinear, finally to be succeeded by a regime in which the curvature of the $\delta^*$ growth is sufficient to approximate a completely contoured nozzle with the source flow turned roughly parallel to the nozzle axis and with a reasonable degree of uniformity restored in the core. With demarcations roughly at $P_{o1}$ = 180 and 700 mm Hg, three regimes consistent with this hypothesis can be observed in Fig. 4. Additional supporting experimental evidence lies in the fact that flow angles measured for the uniform core regime below $P_{o1}$ = 180 mm Hg are only 30 to 50 percent of source flow angles. Lastly, a flow-field calculation by the method of characteristics (Ref. 8), for a conical nozzle corrected by a large calculated $\delta^*$ growth, has yielded core flow Mach number distributions consistent with the pressure distributions of Fig. 4.

### 3.1.3 Mach Number Calibration

Equivalence of two Mach numbers determined separately from the ratios $P_{o2}/P_{o1}$ and $P_1/P_{o1}$ is usually considered ample proof of isentropic flow conditions. In Fig. 5, it is shown that there is reasonable agreement of these Mach numbers above $P_{o1}$ = 45 mm Hg and a marked divergence below this pressure, which is obviously the merge point. Taking care to use $P_{o2}$ at the edge of the core for the non-uniform regime above $P_{o1}$ = 180 mm Hg, this indication of isentropic flow was found from the merge point to the highest reservoir pressure employed. The minimum static pressure in this well established calibraton is 1.5$\mu$. The static temperatures obtained from this calibration are from 8 to 16°K, approximately 23°K below the equilibrium saturation curve for nitrogen. In view of the demonstrated isentropic nature of the nozzle expansion process, there is no doubt that this large degree of supersaturation was actually attained. This propensity of a low density expansion for large degrees of supersaturation was previously noted for $CO_2$ (Ref. 6) and is the result of extremely low nucleation rates at low density. A comparison with a recent correlation of experimental supersaturation data in air (Ref. 9) shows that the present calibration data are clearly in a pressure and temperature regime where no condensation is to be expected.

### 3.1.4 Rarefaction Performance

Referring to Fig. 2, it is shown that the Reynolds number and Knudsen number data obtained from the calibrated nozzle performance do in fact fall on the attainable side of the limiting curves for the adiabatic wall condition. Further, the last experimental point, which is the merge point, agrees quite well with the limit curves. For this nozzle, the maximum $Kn_{cm}$, or maximum mean free path, obtained at the merge point with $T_{o1}$ = 300°K is 0.056 cm. To calculate either $Re_L$ or $Kn_{cm}$ required viscosity values for nitrogen for temperatures down to 8°K. There is no reason why a molecular encounter should be any different below the saturation curve than above it, as long as there is no significant clustering or nucleation, even for very large supersaturations. Based on this reasoning, nitrogen viscosity was calculated using the reduced collision integrals for the Lennard-Jones (6-12) potential and the molecular constants for nitrogen given by Hirschfelder et al. (Ref. 10). It was necessary to extrapolate the collision integrals below 25°K. This calculation is considered more accurate than a Sutherland law for these low temperatures.

## 3.2 $T_{o_1}$ = 300°K WITH CRYOPUMPING WALLS

### 3.2.1 Pitot Pressure Profiles

The effect on the pitot pressure profile of chilling the nozzle walls to 20°K and establishing an effective wall suction by freezing part of the flowing gas to the wall is given in Fig. 6. This particular profile is for the reservoir pressure which gives a merged profile without suction, but the general shape of the cryopumped pitot profiles is quite insensitive to $P_{o1}$. There is, however, a slow variation of both level and core size with $P_{o1}$. There is no well defined core boundary for these profiles, so an effective useful core is defined as that extent of the flow in which the pitot pressure variation is no more than ±5 percent.

### 3.2.2 Mach Number Calibration

The centerline Mach number obtained from the pitot pressure ratio $P_{o2}/P_{o1}$ is given in the uppermost curve of Fig. 5. The probe Reynolds number was low enough for these data that viscous corrections to the measured impact pressure were required and the data of Kosterin et al. (Ref. 11) were used. Correction factors as high as 2.0 were required. Acceptance of this Mach number, based on the single pressure ratio, requires the assumption of isentropic flow on the centerline. This assumption is not as well founded as it is for the adiabatic wall case, because of difficulties in accurately measuring $P_1$. The static pressure

orifice is located in a Plexiglas® ring on which there is no pumping action. Above $P_{o1}$ = 100 mm Hg there is agreement of measured static pressure, corrected for thermal transpiration, with static pressure inferred from the pitot pressure Mach number within a scatter of about 0.3$\mu$. This is sufficient to rule out any large changes in entropy, e.g., from liquefaction in the stream. Below $P_{o1}$ = 100 mm Hg, however, the absolute magnitude of $P_1$ becomes so low that its measurement with available sensors is questionable. In this range, reliance must be placed on the intuitive notion that if wall cryopumping does not change the entropy of the residual nozzle flow above $P_{o1}$ = 100 mm Hg, there is no reason to suppose that it will below.

Removal of a certain fraction of the mass flow from the stream increases the effective area ratio of expansion of the remaining stream and leads to the significant increase in Mach number shown in Fig. 5. The mass flow to the wall has been calculated in two ways: integration of the pitot pressure profile to obtain the residual mass flow and by an independent calculation of the mass flux distribution along the nozzle, based on free-molecule cryopumping conditions with a sticking fraction of 0.87. The results show that at $P_{o1}$ = 76 mm Hg, about 27 percent of the initial mass flow is cryopumped to the nozzle wall.

#### 3.2.3 Rarefaction Performance

Referring to Fig. 2 again, the experimental $Re_L$ and $Kn_{cm}$ for the cryopumping wall mode of operation represent at least an order of magnitude improvement in the rarefaction performance of the nozzle. The experimental total Reynolds number points are lower than the theoretical adiabatic wall limit for the entire range covered, and over at least the lower half of this range, they are lower than the highly cooled wall limit - by a full order of magnitude for the last point at M = 17. The same general remarks apply to the $Kn_{cm}$ data in the lower half of Fig. 2. It can be seen that the longest mean free path attained was 1.75 cm at a Mach number for which the theoretical cold wall nozzle limit is 0.134 cm and the adiabatic wall limit is only 0.023 cm.

This comparison is not complete since the usable core size also varies for all the data shown. A better comparison is shown in the form of $Kn_{cm}$ versus usable core diameter in Fig. 7. The curve for the adiabatic wall case shows the variation of $Kn_{cm}$ within the core for the non-uniform core regime above $P_{o1}$ = 180 mm Hg. Not only is the increased mean free path capability brought out in this plot, but also the accompanying appreciable increase in core size. At the point of vanishing core for the adiabatic wall (at $L_{mean}$ = 0.056 cm), the cryopumped wall provides a core diameter of 2.4 in. Operation at the lowest density obtained in the cryonozzle provides a mean free path of 1.75 cm in a 4.2-in.-diam core.

## 3.3 RESULTS AT HIGH STAGNATION ENTHALPY

### 3.3.1 Boundary Layer Control

No fundamental differences have been found in the aerodynamics of this apparatus when the nitrogen supply is heated up to 4000°K with the arc heater. Although a nominal 40-kw heater is provided, only 2 or 3 kw is put into the gas entering the nozzle. This does represent a large increase in heat load on the cryopump, but the condensate surface area is apparently large enough to maintain reasonable flux levels on the condensate side. Of equal importance, the vent system has proved large enough to handle the increased flow of evolved gaseous hydrogen. The pitot pressure profiles at elevated $T_{o1}$ are similar to the room temperature profiles at corresponding Reynolds number. The variation of useful core size with $T_{o1}$, shown in Fig. 8, indicates a decrease in nozzle wall cryopumping speed as $T_{o1}$ increases. More important, there is a time dependency appearing at high $T_{o1}$ (not shown in Fig. 8) which was not encountered at room temperature. The data of Fig. 8 were obtained within 5 or 6 minutes of the initiation of the flow. At greater time intervals, the core size was observed to decrease gradually towards the no suction values, indicating a gradual fall-off in pumping speed with time. The sensitivity of the cryopumping sticking fraction (and hence pumping speed) to the temperature of the surface of the condensate layer has been shown by Collins and Dawson (Ref. 12). Apparently, the decay in pumping speed is the result of the increasing condensate surface temperature as the condensate thickness increases with time. Since the surface temperature rise is proportional to the heat load, the rise is much more rapid at high stagnation temperature levels.

### 3.3.2 Alternate High Temperature Approaches

Since the degradation of pumping speed at high $T_{o1}$ is the result of the high heat load across the cryodeposit, it is obvious that relief lies in the direction of reducing this heat load. The indirect cryopumping configuration with a porous wall nozzle, investigated by Bottorf and Rogers (Ref. 7), could be adapted to this end by placing liquid nitrogen precooling surfaces between the porous wall of the nozzle and the ultimate cryogenic pumping surfaces. However, these cooling surfaces would also further increase the pressure drop between the base of the boundary layer in the nozzle and the pumping surfaces. A design optimization of the pore configuration and cooling vane configuration would appear to be required. The pore configuration investigated by Bottorf and Rogers yielded Mach number increases of only 0.6 to 1.0, considerably less than the directly pumped nozzle reported herein.

A technique of relieving the heat load on the cryodeposit in the directly pumped nozzle is to cool the boundary layer as much as possible upstream of the surfaces intended to do the pumping. A preliminary indication of the potential of this technique is shown in Fig. 8 for a single data point obtained with the throat section cooled with liquid nitrogen rather than water. A very promising increase in core size is seen, but it proved to be very difficult to maintain a liquid nitrogen flow around the throat. The high heat transfer rates in this region led to a quite rapid gasification of the nitrogen and subsequent vapor lock in the narrow throat cooling passages. A modification to be investigated will consist of water cooling the throat to about the M = 1.5 station, followed by liquid nitrogen cooling from that point to the beginning of the cryopumping section.

### 3.3.3 Evidence of Nitrogen Atoms in Cryodeposit

A startling green luminous glow was observed emanating from the cryodeposits upon initial operation with the arc heater. The glow was quite intense and decayed 20 sec after arc extinguishment. Analysis of this glow showed it to be remarkably simple spectrally: a sharply defined doublet or triplet at 5230 Å and three moderately strong but diffuse lines between 5550 and 5657 Å. Nothing more could be recorded for reasonable plate exposure. A literature search revealed excellent agreement between these lines and the strongest features of spectra previously observed from nitrogen cryodeposits (Refs. 13 and 14). According to these references the glow is from an electronic transition in nitrogen atoms trapped in the cryodeposit. The transition is from the $2P^3 {}^2D$ state to the $2P^3 {}^4S$ ground state - a highly forbidden transition in the normal gaseous state, with a half-life of 20 hr. In the solid matrix this transition becomes highly probable, with a half-life of 15 sec, because of the perturbing effect of the electric quadrupole moments of the closest neighboring nitrogen molecules.

From the gas dynamic standpoint, this phenomenon is interesting because it indicates a lack of equilibrium in the nozzle reservoir. Departures from equilibrium are to be expected in high temperature, low density nozzle expansions, but it is usually assumed that the starting condition is at equilibrium, because of the long particle residence time there. These glows have been observed (hence implying atoms surviving the journey from arc column to cryopump) for reservoir conditions as low as 1000°K and up to 1/2 atmosphere of pressure. The mass fraction involved in producing these glows is not known at the present time.

## SECTION IV
## CONCLUSIONS

1. For room stagnation temperature, the control of low density boundary layers in nozzles by direct cryopumping to the walls gives an order of magnitude increase in the degree of rarefaction attainable in a hypersonic nozzle.

2. The effectiveness of the wall cryopumping falls off at elevated stagnation temperatures, but some degree of effectiveness is retained even at 4000°K. A time dependency is also felt through pumping speed decrease as condensate surface temperature rises. Nevertheless, 5- or 6-min runs are still possible at $T_{o1}$ = 4000°K before any appreciable loss in performance is encountered.

3. Preliminary evidence has been found that the performance decay at high $T_{o1}$ may be alleviated by precooling the suction flow - either by use of highly cooled walls ahead of the cryopumping section or by the introduction of intercooling in an indirectly cryopumped porous-wall nozzle.

4. A certain number of atoms produced in the arc column of the arc heater survive not only the nozzle recombination process, but also resist recombination in the nozzle reservoir at moderately low temperatures (~1000°K). They are ultimately imbedded in the cryodeposit in free radical form, where their presence is demonstrated by a luminous green glow with spectral characteristics of an electronic transition in nitrogen atoms.

## REFERENCES

1. Chuan, R. L., Springer, L. M., and Waiter, S. A. "Operation and Calibration of the Low Density Wind Tunnel." USCEC 56-215, Univ. Sou. Calif. Eng. Center, July 1960.

2. Van Driest, E. R. "Investigation of Laminar Boundary Layer in Compressible Fluids Using the Crocco Method." NACA TN 2597, January 1952.

3. Stalder, J. R., Goodwin, G., and Creager, M. O. "Heat Transfer to Bodies in a High-Speed Rarefied-Gas Stream." NACA Report 1093, 1952.

4. Enkenhus, K. R. "The Design, Instrumentation and Operation of the UTIA Low Density Wind Tunnel." UTIA 44, University of Toronto, June 1957.

5. Chuan, R. L. and Krishnamurty, K. "Principle and Application of Two-Phase Wind Tunnel System, Interim Report." USCEC 42-201, Univ. Sou. Calif. Eng. Center, December 1955.

6. MacDermott, W. N. "Preliminary Experimental Results of the Reduction of Viscous Effects in a Low Density Supersonic Nozzle by Wall Cryopumping." AEDC-TN-61-71 (AD264656), October 1961.

7. Bottorf, M. R. and Rogers, K. W. "Theoretical and Experimental Investigation of Boundary Layer Control in Low-Density Nozzles by Wall Suction and Cooling." USCEC 90-101, Univ. Sou. Calif. Eng. Center, March 1963.

8. Jacocks, J. L., ARO, Inc. Private Correspondence, 1964.

9. Daum, F. L. "The Condensation of Air in a Hypersonic Wind Tunnel." AIAA Journal, Vol. I, No. 5, May 1963.

10. Hirschfelder, J. O., Curtiss, C. F., and Bird, R. B. Molecular Theory of Gases and Liquids. John Wiley & Sons, Inc., New York, 1954.

11. Kosterin, S. I., Yushchenkova, N. I., Belova, N. T., and Kamaev, B. D. "An investigation into the Effect of the Rarefaction of a Supersonic Stream on the Readings of a Total-Head Probe." Int. Chem. Eng., Vol. III, No. 2, April 1963.

12. Collins, J. A. and Dawson, J. P. "Cryopumping of 77°K Nitrogen and Argon on 10-25°K Surfaces." AEDC-TDR-63-51 (AD404174), May 1963.

13. Bass, A. M. and Broida, H. P. "Spectra Emitted from Solid Nitrogen Condensed at 4.2°K from Gas Discharge." Phys. Rev., Vol. 101, Part 6, March 1956.

14. Herzfeld, C. M. "Theory of Forbidden Transitions of Nitrogen Atoms Trapped in Solids." Phys. Rev., Vol. 107, Part 5. September 1957.

15. Sreekanth, A. K. "Drag Measurements on Circular Cylinders and Spheres in the Transition Regime at a Mach Number of 2." UTIA 74, University of Toronto, April 1961.

16. Potter, J. L., Kinslow, M., Arney, G. D., and Bailey, A. B. "Description and Preliminary Calibration of a Low Density, Hypervelocity Wind Tunnel." AEDC-TN-61-83 (AD262466), August 1961.

17. Wegener, P. P. and Ashkenas, H. "Wind Tunnel Measurements of Sphere Drag at Supersonic Speeds and Low Reynolds Number." J. Fluid Mech., Vol. X, No. 4, June 1961.

18. Chuan, R. L. "Research on Rarefied Gasdynamics and Plasmadynamics." USCEC 83-101, Univ. Sou. Calif. Eng. Center, September 1962.

19. Emerson, D. E. and Schaaf, S. A. "Performance of a Supersonic Nozzle in the Rarefied Gas Dynamics Regime." Univ. Calif. Report He-150-72 (ATI 135417), August 1950.

20. Maslach, G. J. and Sherman, F. S. "Design and Testing of an Axisymmetric Hypersonic Nozzle for a Low Density Wind Tunnel." WADC-TR-56-341, August 1956.

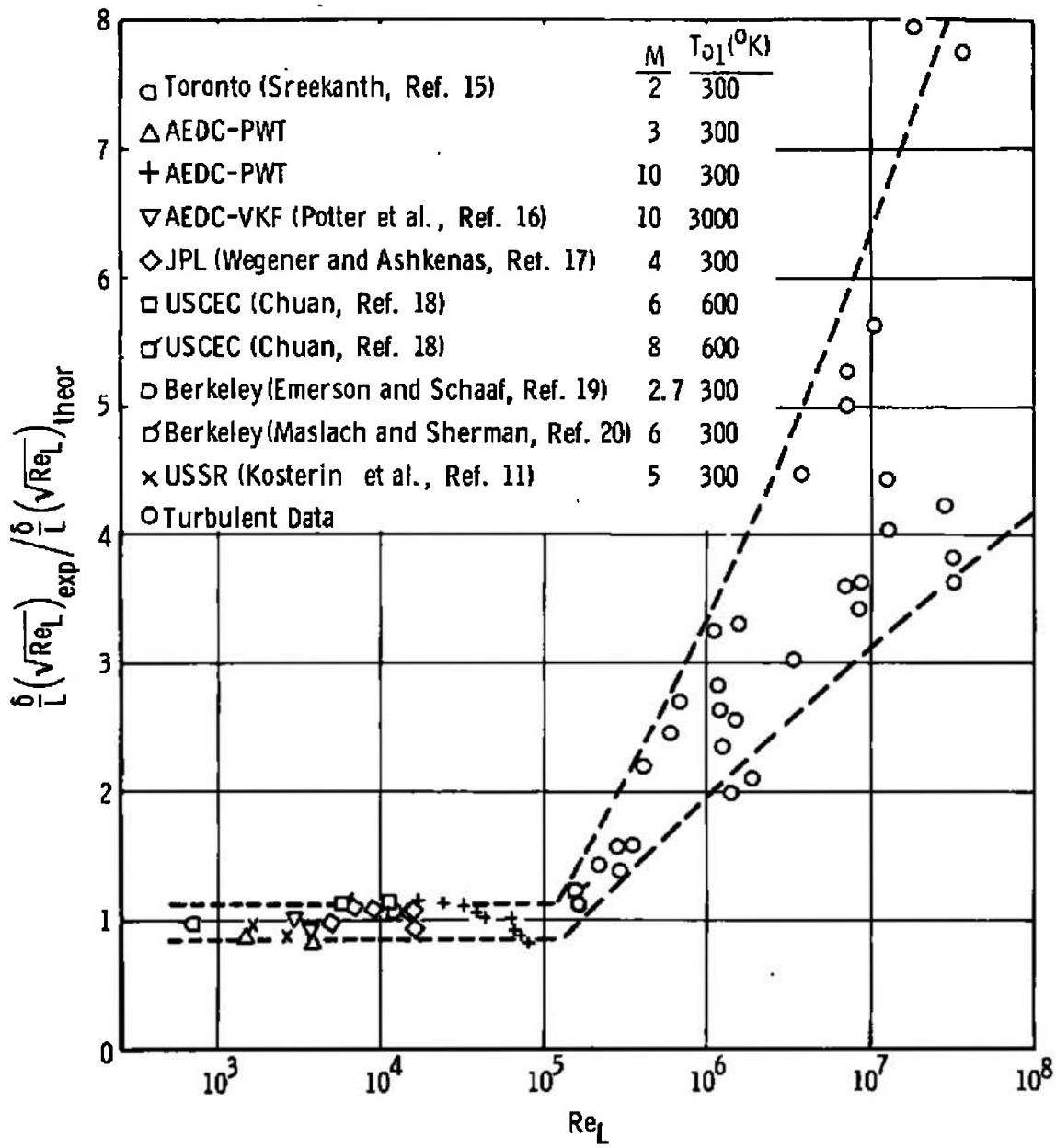


**Fig. 1 Correlation of Experimental Nozzle Boundary-Layer Thicknesses with Laminar Flat Plate Theory**

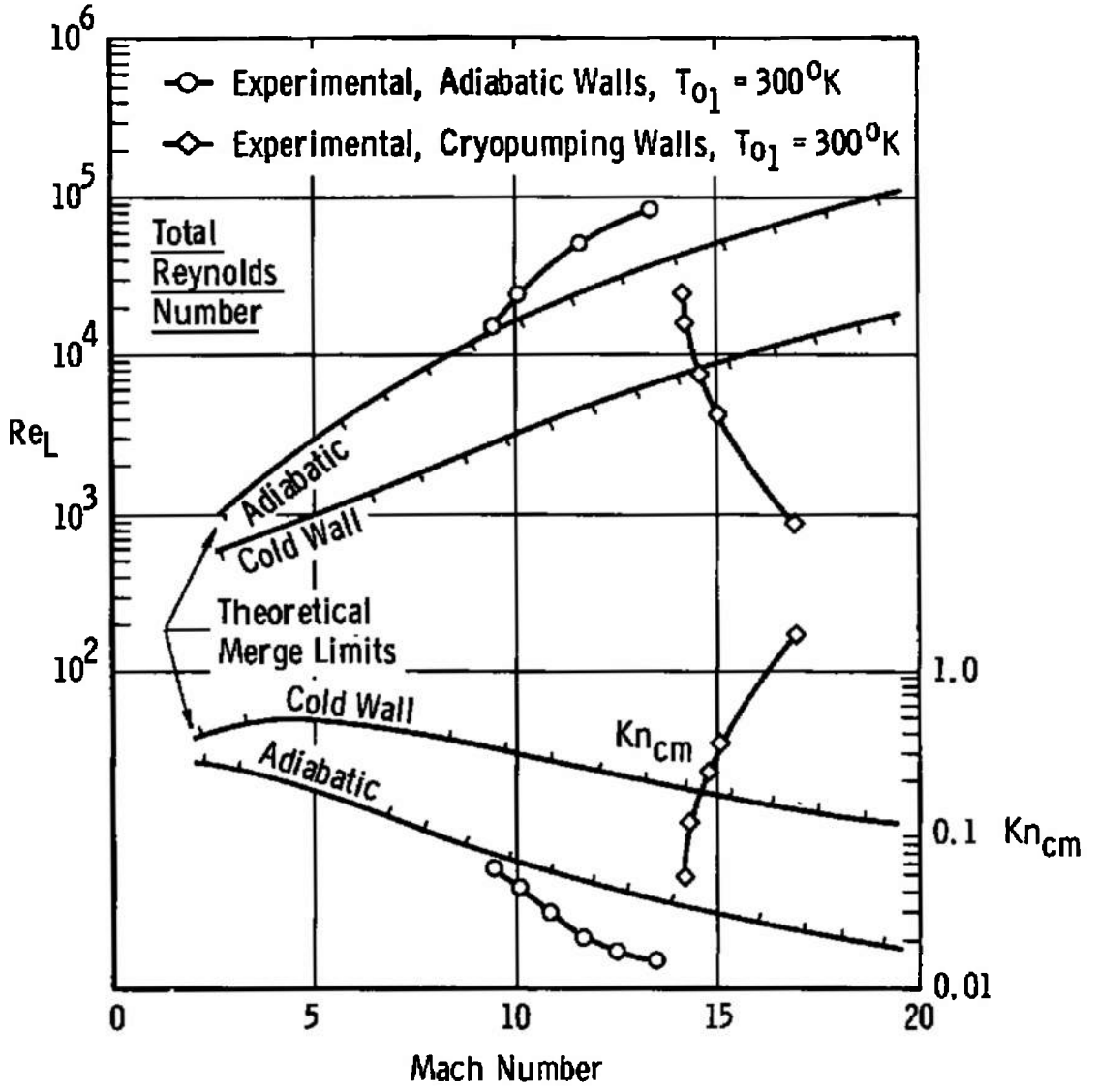


Fig. 2 Comparison of Experimental Total Reynolds Number and Knudsen Number with Theoretical Limits for a 1-ft-diam Hypersonic Nozzle with L/D = 2.0

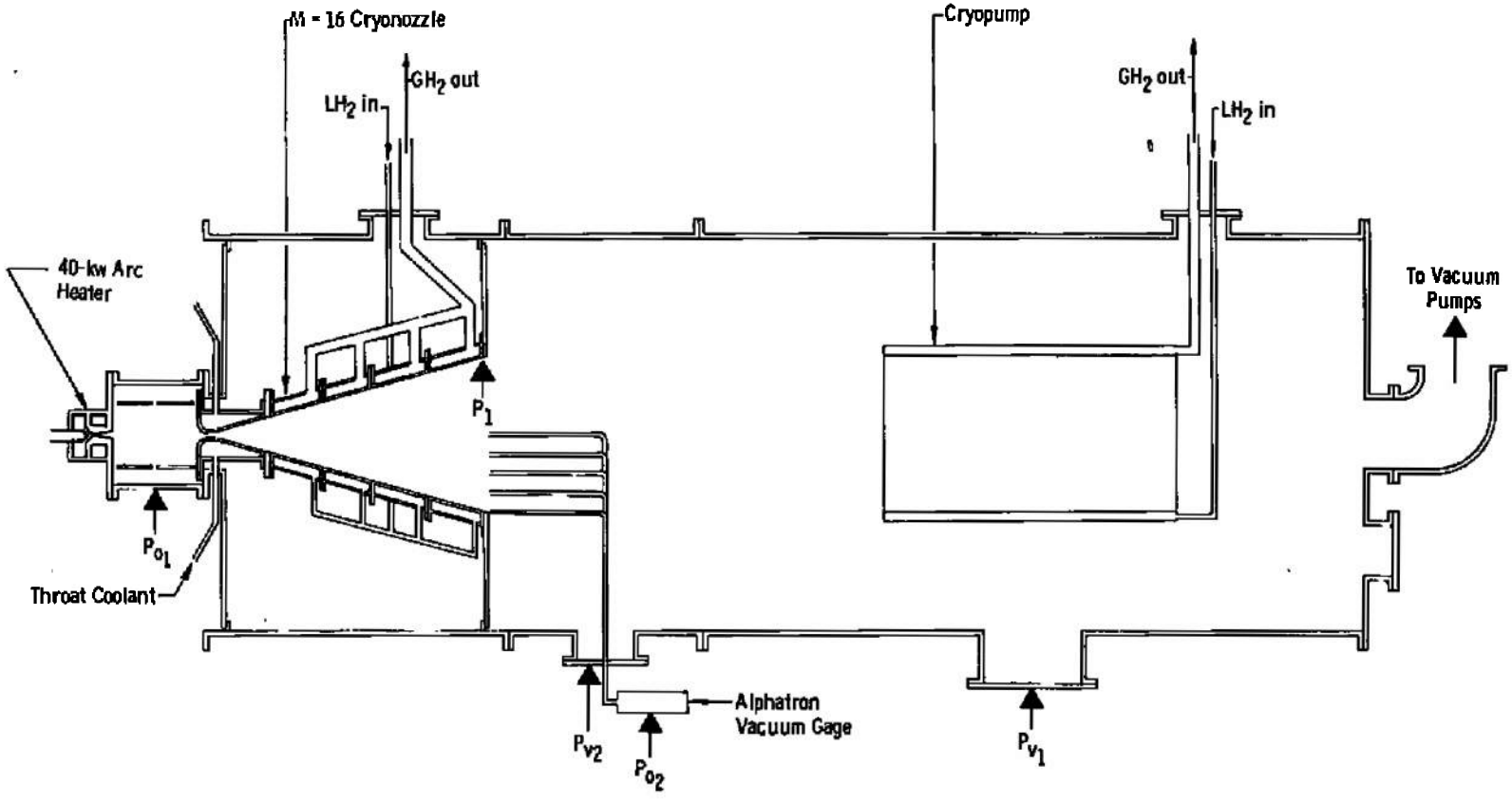


**Fig. 3 Low Density Boundary Layer Control Tunnel Configuration**

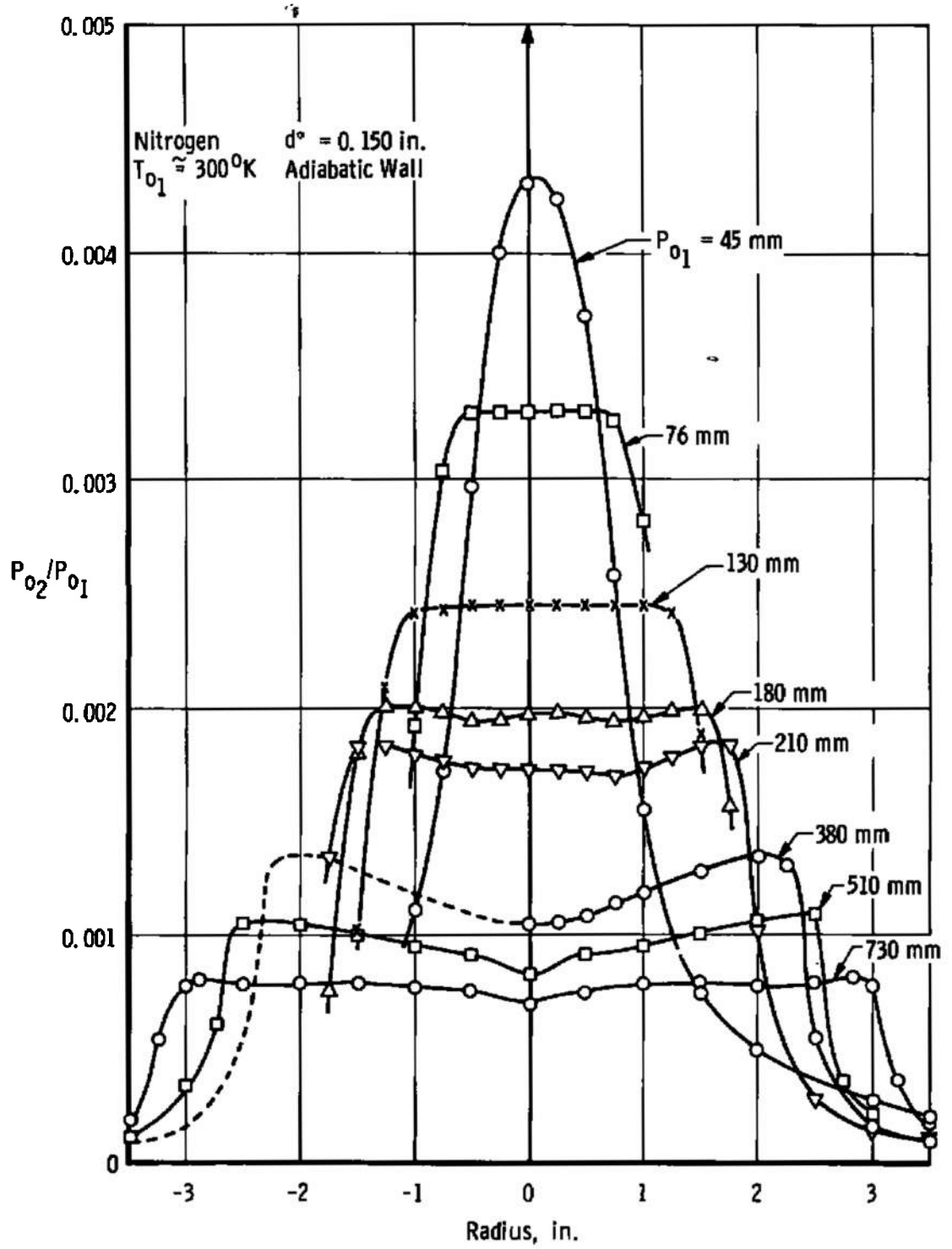


Fig. 4 Pitot Pressure Profiles at Various Reservoir Pressures

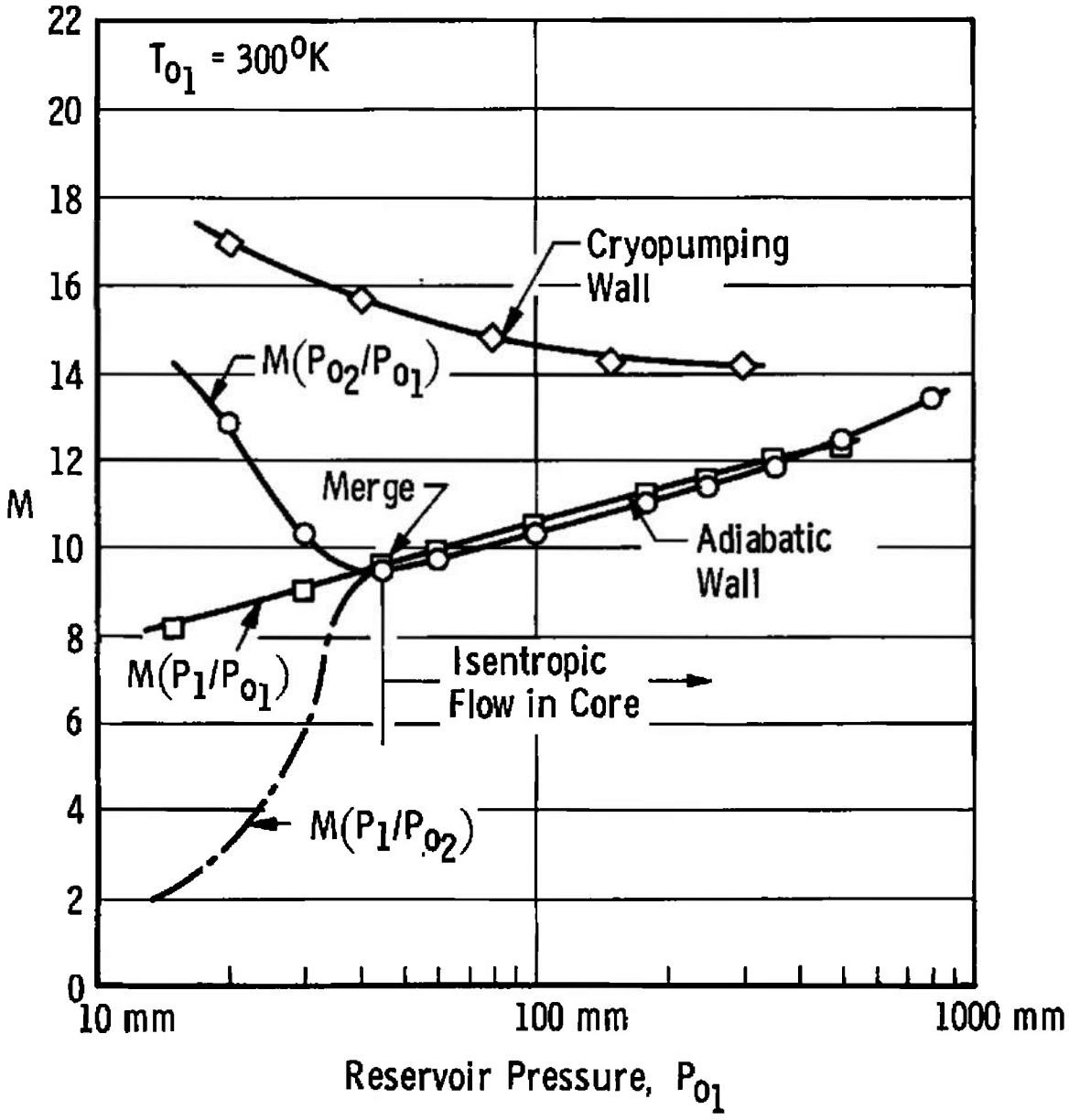


Fig. 5 Mach Number versus Reservoir Pressure with and without Suction

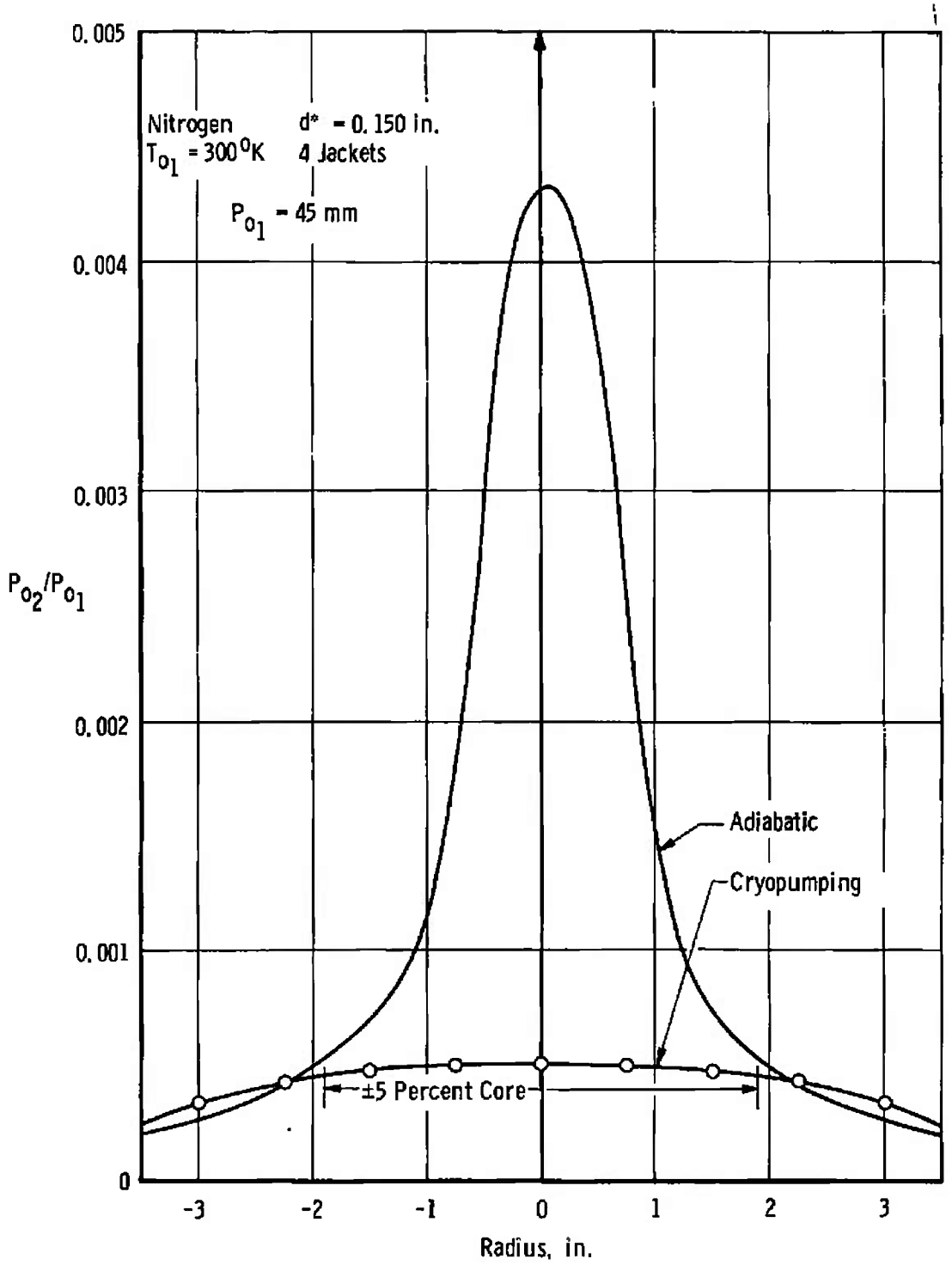


**Fig. 6 Effect of Wall Cryopumping on Pitot Pressure Profile**

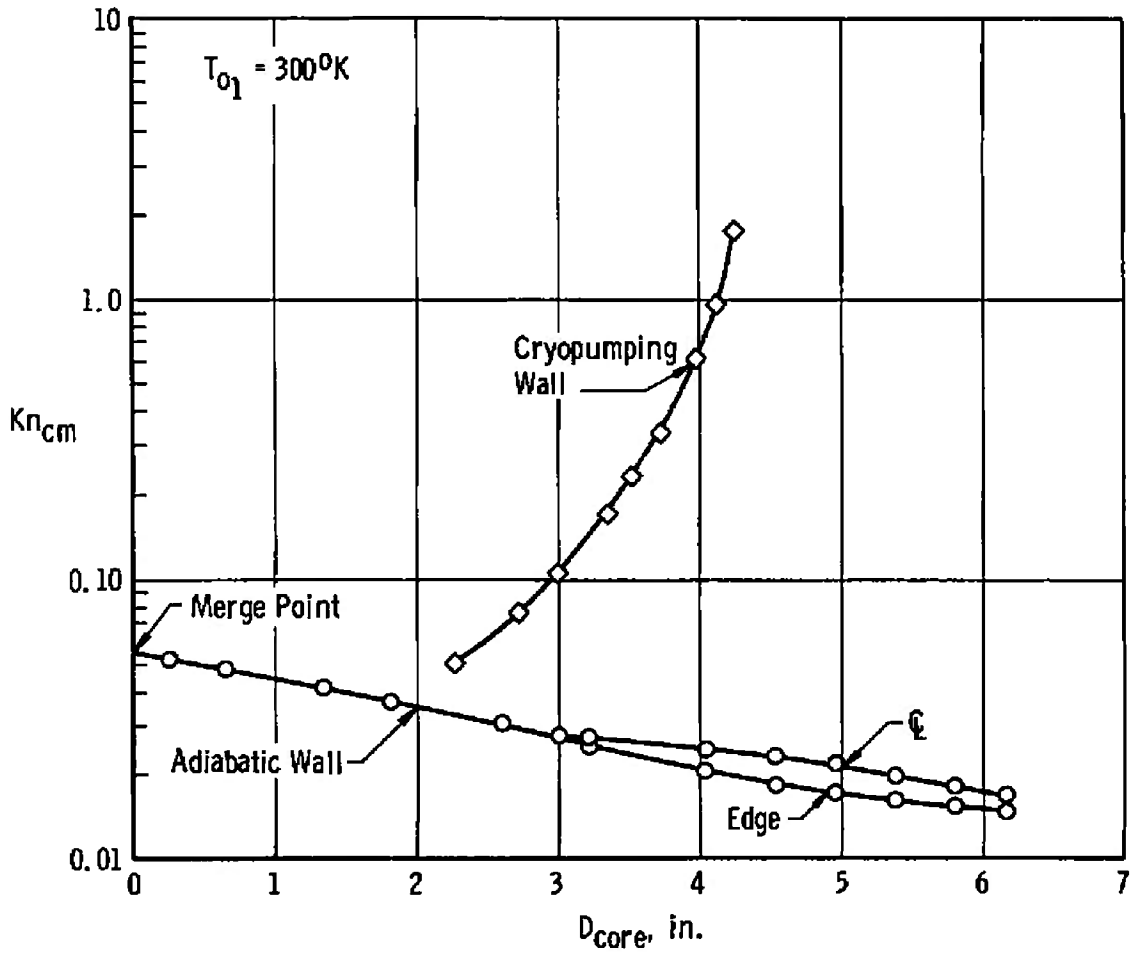


Fig. 7 Knudsen Number for 1 cm Characteristic Length versus Core Diameter

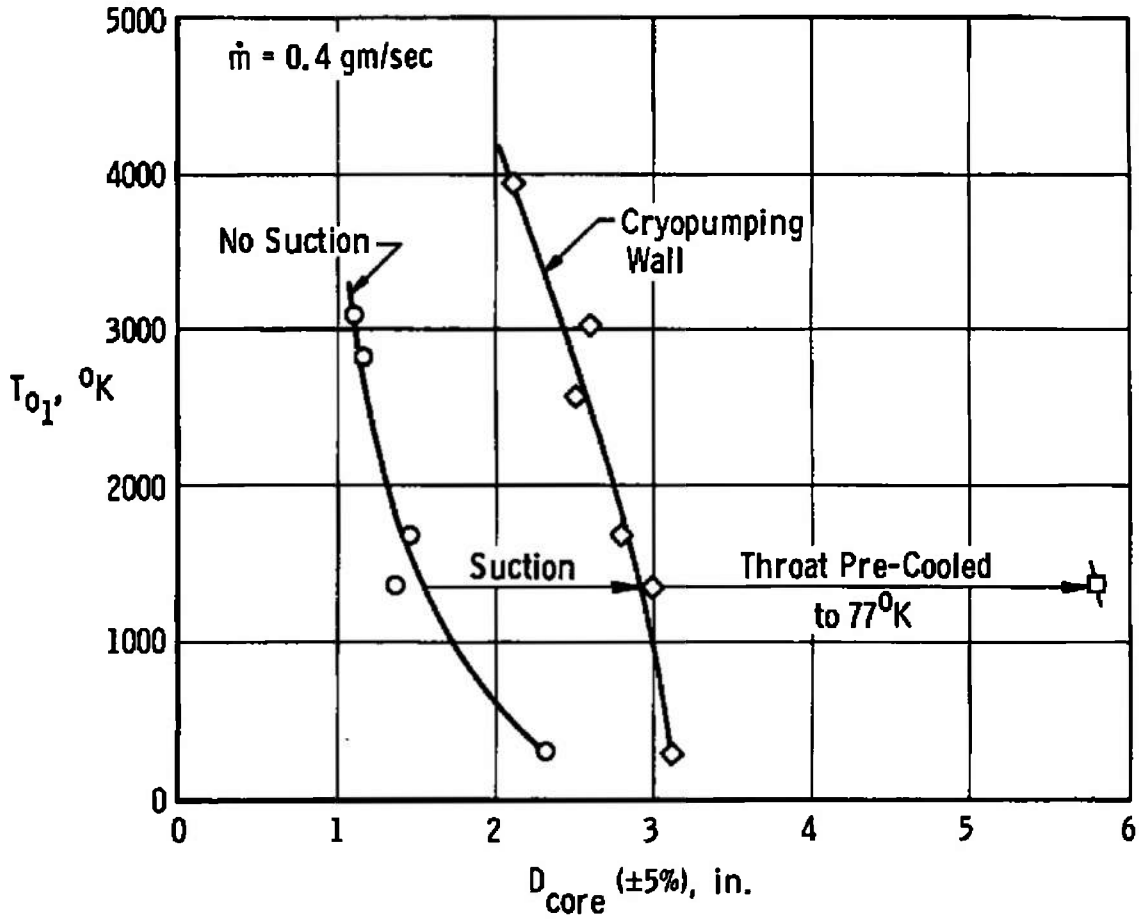


Fig. 8 Effect of Stagnation Temperature on Core Size, $\dot{m}$ = 0.4 gm/sec

UNCLASSIFIED

Security Classification

**DOCUMENT CONTROL DATA - R&D**

*(Security classification of title, body of abstract and indexing annotation must be entered when the overall report is classified)*

1 ORIGINATING ACTIVITY *(Corporate author)*
Arnold Engineering Development Center
ARO, Inc., Operating Contractor
Arnold AF Station, Tennessee

2a REPORT SECURITY CLASSIFICATION
UNCLASSIFIED

2b GROUP
N/A

3 REPORT TITLE
LOW DENSITY BOUNDARY LAYER CONTROL BY LIQUID HYDROGEN CRYOPUMPING

4 DESCRIPTIVE NOTES *(Type of report and inclusive dates)*
N/A

5 AUTHOR(S) *(Last name, first name, initial)*
MacDermott, W. N., Dix, R. E., and Shirley, B. H., ARO, Inc.

| 6 REPORT DATE | 7a. TOTAL NO. OF PAGES | 7b. NO. OF REFS |
|---|---|---|
| August 1965 | 28 | 20 |

8a. CONTRACT OR GRANT NO.
AF 40(600)-1200

b. PROJECT NO.
7778

c.
Program Element 62410034

d.

9a. ORIGINATOR'S REPORT NUMBER(S)
AEDC-TR-65-148

9b. OTHER REPORT NO(S) *(Any other numbers that may be assigned this report)*
N/A

10. AVAILABILITY/LIMITATION NOTICES
Qualified requesters may obtain copies of this report from DDC.

11. SUPPLEMENTARY NOTES
N/A

12. SPONSORING MILITARY ACTIVITY
Arnold Engineering Development Center
Air Force Systems Command
Arnold AF Station, Tennessee

13 ABSTRACT

Boundary layers in a low density wind tunnel nozzle have been reduced by applying suction on the diverging walls of the nozzle and by cryogenically pumping the boundary layer gas directly to the wall. The experimental apparatus used in this study incorporates a 12-in.-diam hypersonic nozzle and a 16-in. primary liquid hydrogen cryopump with a pumping speed of 200,000 liters/sec. Comparison of pitot and static pressures measured in this nozzle with nitrogen at 300°K indicates a supersaturated isentropic flow regime bounded on the low pressure end by a merged boundary layer. In a typical operating condition (upstream temperature of 300°K) a merged boundary layer flow at M = 9.50, Re = 256/cm, and a mean free path of 0.06 cm was converted to a 4-in. core flow with M = 15.7, Re = 40/cm, and a mean free path of 0.6 cm by cooling the nozzle walls sufficiently for cryopumping. The wall cryopumping retains effectiveness at supply temperatures at least as high as 4000°K.



DD FORM 1 JAN 64 1473

UNCLASSIFIED

Security Classification

| 14 KEY WORDS | LINK A | | LINK B | | LINK C | |
|---|---|---|---|---|---|---|
| | ROLE | WT | ROLE | WT | ROLE | WT |
| Wind Tunnels<br>Low Density<br>Boundary Layer Removal<br>Cryogenics<br>Liquid Hydrogen<br>Hypersonic Flow | | | | | | |

## INSTRUCTIONS

1. ORIGINATING ACTIVITY: Enter the name and address of the contractor, subcontractor, grantee, Department of Defense activity or other organization *(corporate author)* issuing the report.

2a. REPORT SECURITY CLASSIFICATION: Enter the overall security classification of the report. Indicate whether "Restricted Data" is included. Marking is to be in accordance with appropriate security regulations.

2b. GROUP: Automatic downgrading is specified in DoD Directive 5200.10 and Armed Forces Industrial Manual. Enter the group number. Also, when applicable, show that optional markings have been used for Group 3 and Group 4 as authorized.

3. REPORT TITLE: Enter the complete report title in all capital letters. Titles in all cases should be unclassified. If a meaningful title cannot be selected without classification, show title classification in all capitals in parenthesis immediately following the title.

4. DESCRIPTIVE NOTES: If appropriate, enter the type of report, e.g., interim, progress, summary, annual, or final. Give the inclusive dates when a specific reporting period is covered.

5. AUTHOR(S): Enter the name(s) of author(s) as shown on or in the report. Enter last name, first name, middle initial. If military, show rank and branch of service. The name of the principal author is an absolute minimum requirement.

6. REPORT DATE: Enter the date of the report as day, month, year; or month, year. If more than one date appears on the report, use date of publication.

7a. TOTAL NUMBER OF PAGES: The total page count should follow normal pagination procedures, i.e., enter the number of pages containing information.

7b. NUMBER OF REFERENCES: Enter the total number of references cited in the report.

8a. CONTRACT OR GRANT NUMBER: If appropriate, enter the applicable number of the contract or grant under which the report was written.

8b, 8c, & 8d. PROJECT NUMBER: Enter the appropriate military department identification, such as project number, subproject number, system numbers, task number, etc.

9a. ORIGINATOR'S REPORT NUMBER(S): Enter the official report number by which the document will be identified and controlled by the originating activity. This number must be unique to this report.

9b. OTHER REPORT NUMBER(S): If the report has been assigned any other report numbers *(either by the originator or by the sponsor)*, also enter this number(s).

10. AVAILABILITY/LIMITATION NOTICES: Enter any limitations on further dissemination of the report, other than those imposed by security classification, using standard statements such as:

(1) "Qualified requesters may obtain copies of this report from DDC."

(2) "Foreign announcement and dissemination of this report by DDC is not authorized."

(3) "U. S. Government agencies may obtain copies of this report directly from DDC. Other qualified DDC users shall request through _____."

(4) "U. S. military agencies may obtain copies of this report directly from DDC. Other qualified users shall request through _____."

(5) "All distribution of this report is controlled. Qualified DDC users shall request through _____."

If the report has been furnished to the Office of Technical Services, Department of Commerce, for sale to the public, indicate this fact and enter the price, if known.

11. SUPPLEMENTARY NOTES: Use for additional explanatory notes.

12. SPONSORING MILITARY ACTIVITY: Enter the name of the departmental project office or laboratory sponsoring *(paying for)* the research and development. Include address.

13. ABSTRACT: Enter an abstract giving a brief and factual summary of the document indicative of the report, even though it may also appear elsewhere in the body of the technical report. If additional space is required, a continuation sheet shall be attached.

It is highly desirable that the abstract of classified reports be unclassified. Each paragraph of the abstract shall end with an indication of the military security classification of the information in the paragraph, represented as *(TS), (S), (C), or (U)*.

There is no limitation on the length of the abstract. However, the suggested length is from 150 to 225 words.

14. KEY WORDS: Key words are technically meaningful terms or short phrases that characterize a report and may be used as index entries for cataloging the report. Key words must be selected so that no security classification is required. Identifiers, such as equipment model designation, trade name, military project code name, geographic location, may be used as key words but will be followed by an indication of technical context. The assignment of links, rules, and weights is optional.